

Design and Performance Evaluation of a PEM Fuel Cell – Lithium Battery–Supercapacitor Hybrid Power Source for Electric Forklifts

*Chuang-Yu Hsieh, Xuan-Vien Nguyen, Fang-Bor Weng, Tzu-Wei Kuo, Zhen-Ming Huang, Ay Su**

Department of Mechanical Engineering & Fuel Cell Center, Yuan Ze University, Taoyuan 320, Taiwan

*E-mail: meaysu@saturn.yzu.edu.tw

Received: 13 August 2016 / *Accepted:* 11 October 2016 / *Published:* 10 November 2016

In this study, we developed a hybrid power source with a direct current (DC) supply system for electric forklifts. Its designs were based on harsh operating conditions, in line with the requirements for the truck. The power source consists of a fuel cell (FC) system, lithium ion batteries, and supercapacitor modules. This system supplies the pallet truck with the power needed for lifting and moving. In the experiments, three kinds of power source modules were designed, and their performance was tested individually. The modules were then combined and tested using machines to simulate load conditions. The test parameters examined were the rate of the supercapacitor and charging and discharging properties. A final simulation of the overall power output performance was also performed. The power output may be divided into power for lifting and power for moving. The FC is the power source for the traveling motor, while the lithium ion battery is the supply for maximum instantaneous power for the pallet truck. The super capacitors protect the FC and batteries and ensure high power output. It can also offset the insufficiency and instability of the power provided by the first two power sources and provides a stable 24 V DC power supply for the traveling motor when connected to a DC power converter. The lithium ion battery and supercapacitor modules are able to power the lifting motors, which require high power output, providing a maximum instantaneous power of 3.2 kW for several cycles of lifting. The power source proposed here therefore has potential use in hybrid systems.

Keywords: hybrid systems, proton-exchange membrane fuel cells, lithium ion battery, supercapacitor circuits, power management

1. INTRODUCTION

The proton-exchange membrane fuel cell (PEMFC) is an energy storage technology that features room-temperature quick start, zero emission, and high-efficiency energy conversion [1–4].

PEMFCs are used not only for the construction of power stations or as a mobile power source, but also in electric pallet trucks and mobile carriers. General internal combustion engines and battery-powered engines are more developed than is fuel cell (FC) technology despite that FCs offer advantages with respect to environmental protection, long-term charging, and other factors. In its cost assessment of powering load-handling equipment with FCs in accordance with annual usage patterns, the United States Department of Energy found that the cost of FCs can be 10% lower than the cost of lead acid batteries [5, 6]. Nevertheless, the following requirements need to be considered in the use FCs as power source for such equipment: (i) Adaptability to rapid changes: FCs generally lacks this characteristic [7–9], requiring a substantial period to produce their output, whereas handling equipment need instant output. (ii) Overall efficiency: Power management maximizes the efficiency of the FC system [10–14]; whereas the efficiency of internal combustion engines can generally be improved by about 30% using power management, that of FC engines can be improved by up to 60%. Additionally, cogeneration can improve the efficiency of FC engines by 85%. (iii) Hydrogen storage method: Several methods for storing hydrogen exist.

At present, high-pressure hydrogen storage or hydrogen-absorbing metals are used in vehicles. The technology is simple to use and can enable storage of hydrogen at 700–1000 psi. However, legal requirements in Taiwan limit hydrogen storage cylinders in vehicles to a hold a maximum pressure of 150 psi, thereby substantially lowering the vehicle's fuel mileage. Furthermore, the cost of hydrogen storage using metals increases as the vehicular weight increases. To address these limitations, adjusting the center of gravity of load-handling equipment by shifting its weight distribution during cargo transport has been considered. This strategy however has its own advantages and disadvantages. The design takes into account the mode of use to determine the most suitable hydrogen storage method and thus to optimize the vehicle's performance.

At present, lead acid batteries have reached maturity as a power source [15, 16]. This system is easy to obtain, and its technological requirements are low. However, it has a long charging time and the system becomes too large and heavy when constructed in series or in parallel. Lithium batteries have advantages in terms of energy density, operating voltage, output power, and discharge stability, while their disadvantages are the risks of overheating and overcharge during their use [17]. An alternative to the above power sources are FCs, which offer the advantages of quick start and minimal charging downtime. The drawback to this technology, however, is its weak pulse type. Consequently, FCs are combined with lithium batteries and supercapacitors. This approach can reduce the instantaneous tensile load of the FC and can minimize reductions of the FC's wattage. Furthermore, it shortens the operating cycle of the FC, thereby increasing its longevity and reducing its cost, as well as simplifies the control module of the FC. Electric forklifts, in particular, might require the use of supercapacitors; thus, attention should be paid to such application. For operations involving heavy loads, lithium batteries or FCs are inadequate, as they cannot supply large amounts of power. Furthermore, the fast discharge of supercapacitors can lead to stable voltage and current, protects lithium batteries and FCs, and provides other benefits [18–22]. Therefore, studies have aimed at including ultracapacitors in the design of various power supply systems. In contrast to using a single mode, which increases the cost and requirements for improving the power supply, combining two or three power sources greatly improves the power supply and simultaneously minimizes the

disadvantages and cost encountered with the single-mode strategy. Several studies have shown that the energy management system enables combinations of energy sources to perform at high efficiency [23–24].

According to a laboratory study, there will be significant future developments in FC-powered vehicles. Hence, the present study focused on combining the power sources FCs, lithium batteries, and ultracapacitors in order to develop a power system for an electric pallet truck, as well as examined the feasibility and applications of the power system.

2. EXPERIMENTAL

2.1. Assembly of the water-cooled FC stack

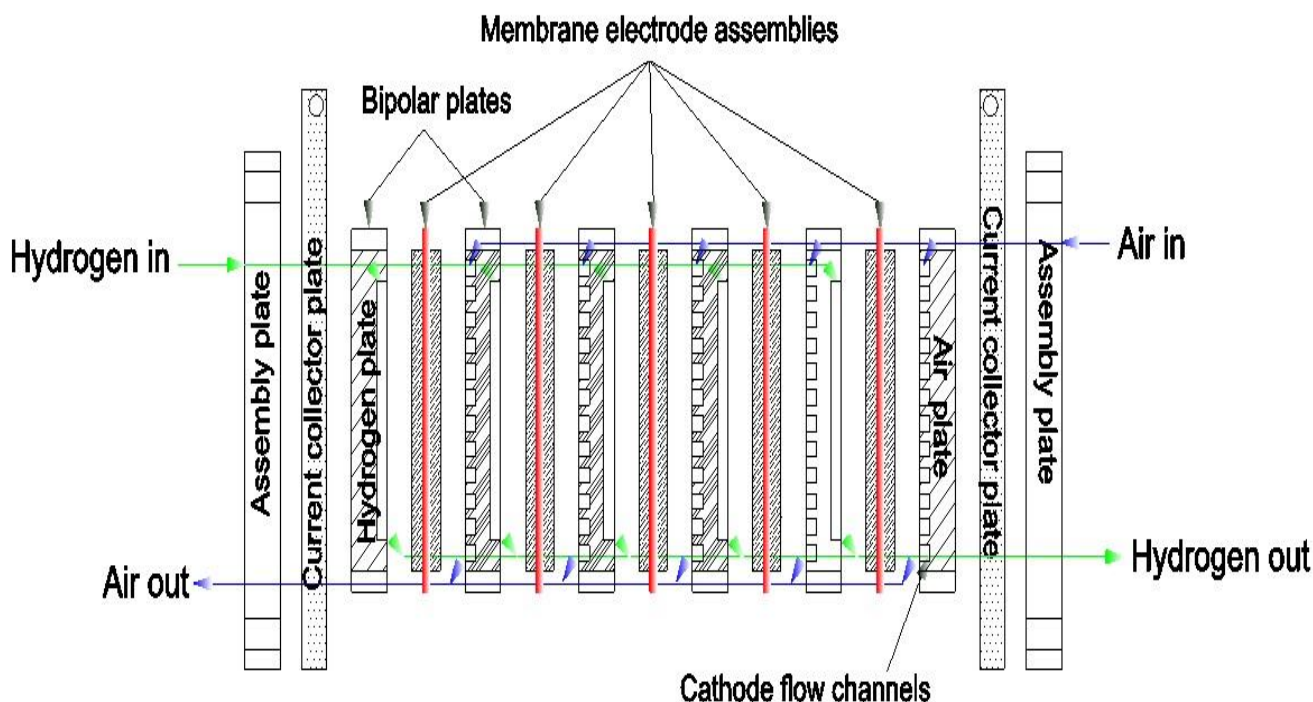


Figure 1. Diagram of the fuel cell (FC) assembly

We created a water-cooled FC stack for the electric pallet truck (Figure 1). The design goal was to achieve a battery output power of 1.5–1.8 kW at 26 V. The bipolar plate stack consists of graphite and has 150 mm width, 150 mm length, and 4 mm height. Each active area of the cell has dimensions of 150 cm². The anode flow channel has 20 parallel channels, with each flow channel having 1 mm height and 1 mm width. The cathode channel has 60 straight parallel channels, each with a 1 mm height and 1 mm width, and the collector plate consists of gold-plated brass. The cell comprises a stack of 40 single batteries. The battery is cooled with circulating water to carry away cell heat generated by the electrochemical reaction. The cathode is supplied with air from a blower controlled by a signal with a voltage of 0–5 V, which is greater than the supply voltage. A greater amount of air supplied

requires a larger amount of air on cathode side. Therefore, the controlling voltage signal is proportional to the load. The stack specifications are listed in Table 1.

The FC stack performance was tested at the 6 kW FC test station at Thai New Energy Company. The tests, which include scanning-voltage, constant-voltage, and constant-current tests, as well as a dynamic-load test, simulate the actual operation. The above tests were conducted to obtain optimal battery operating parameters, as well as to simulate operation of the vehicle in the factory and the change in performance of the FC under different load conditions.

Table 1. Specifications of the water-cooled fuel cell stack

Project	Specification
Stack size	225 mm(length), 155 mm (width), 180 mm (height)
Stack weight	15kg
Reaction area	150 cm ²
Number of Batteries	40
Runner form	20 Snake
Fuel type	H ₂ /Air
Power	2.5kW
Cooling form	Water-cooled

2.2. Design of the auxiliary device for energy storage

The cathode for the lithium battery, also known as the terpolymer lithium battery, consists of nickel, cobalt, and manganese (MnNiCo). It has a nominal voltage of up to 4.2 V, a small size, and a high energy density. The lithium ion battery, on the other hand, has a nominal voltage of 3.6 V. Thus, we monitored the discharge status of the specimens 1C (1100 mA) using a lithium ion battery. The battery, which has discharged properties of 29 V–10 A, had been charged at room temperature and had been allowed to stand for 1h. The discharge properties of specimens 3C and 5C were also measured under the above operating conditions.

The supercapacitor modules for Parts A and B, which have different sizes, are shown in Table 2. In the first module, 13 supercapacitors were connected in series to establish an equivalent 35.1 V circuit with a capacitance of 23 F. Small capacitances are appropriate for hybrid electric power distribution, providing a buffer in the ideal state of the FC space and thus protecting the FC. The instantaneous output of this module does not cause damage and instead enhances the efficiency of the lithium ion batteries. In the second module, 12 supercapacitors were used in series to establish an equivalent circuit of 32.4 V with four groups having a parallel capacitance of 106 F. Motors used for hoisting, which require high currents, also require high capacitance for the output.

Table 2. Specifications for the auxiliary power supply

Project	Specification
Part A	
Lithium battery	VISTA Advance Tech @ NCM-peak 24V / 20Ah / 7S2P
Supercapacitive	13 supercapacitors in series, a string 35.1 V/ 23 F
Part B	
Lithium battery	VISTA Advance Tech @ NCM-peak 24V / 20Ah / 7S2P
Supercapacitive	12 super capacitors in series, 4 parallel group 32.4 V / 106 F

2.3. Design of the test platform for the hybrid system

The configuration of the hybrid system for the electric pallet truck and its power infrastructure are shown in Figure 2. The power required for the vehicle’s motor (traveling motor) is 1.8 kW at 24 V, and the lifting motor requires a power of 2.5 W at 24 V. The vehicle’s modes of operation may be divided into one traveling mode and two lifting modes. (1) Traveling mode (Part A): The FC stack operates at 1.6–2 kW at 26 V and is the main source of power.

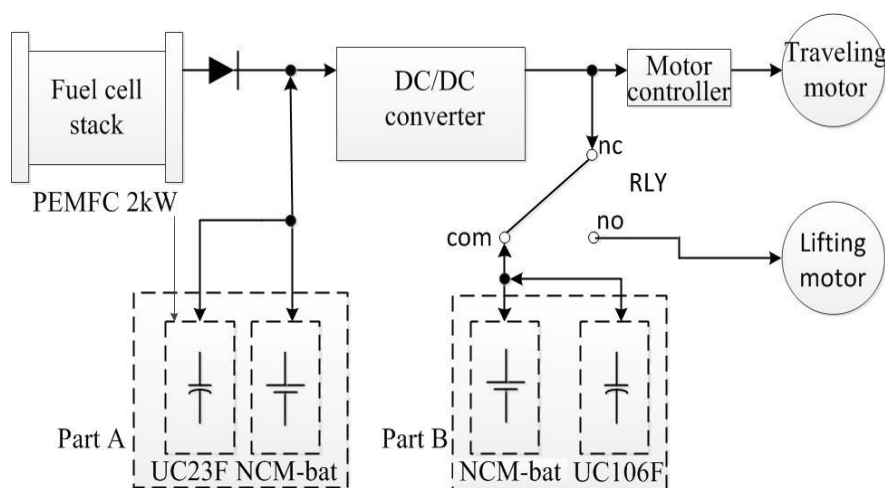


Figure 2. Schematic of the hybrid power management

The auxiliary source of kinetic energy of the device consists of a lithium ion battery operating at 24 V–20 Ah. The supercapacitor (23 F) in parallel is composed of the FC and a parallel connection for the auxiliary source of kinetic energy via the DC/DC power converter. The power supply to the drive motor has a constant output power at a voltage of 29 V, which is transmitted through the auxiliary contacts of the electromagnetic contactor (magnetic contactor). The contactor turns the

control loop for the kinetic energy source. (2) Lifting mode (Part B): During lifting the load end, the magnetic contactor is jump-started in charging mode. Hoisting begins at motor discharge, at which point the output terminal of the DC/DC converter no longer charges. Subsequently, the lifting motor stops, the magnetic contactor immediately reverts to charging mode, and the output terminal of the DC/DC converter charges. Since the DC/DC converter output voltage is fixed at 29 V, Part B provides part of the power and it does not discharge to the traveling motor.

3. RESULTS AND DISCUSSION

3.1. Performance of the water-cooled FC stack

In a separate experiment using an electric pile fabricated in-house, we conducted tests to find the optimum parameters for the stack. Tests were conducted on (i) the dose of hydrogen, (ii) the air stoichiometric ratio, (iii) the temperature, and (iv) the stack performance. Normally, the fuel cell limited current or power slope has been experimentally determined as the highest slope of operated fuel cell system, where no fuel starvation occurs, for example, 4 As^{-1} for a 0.5 kW, 12.5 V PEMFC [25]; and a 2.5 kW s^{-1} for a 40 kW, 70 V PEMFC [26]. Supercapacitor is the highest dynamic power source, which provides the micro-cycles and the fast dynamic power supply. Battery is between fuel cell and supercapacitor in the dynamic classification. There are many possible structures to connect a main power source and two storage devices with the utility DC bus. The total mass, volume, cost and efficiency of the propulsion system are investigated. It is composed of a unidirectional converter (step-up converter) for a fuel cell stack, bidirectional (2-quadrant) converters for battery and supercapacitor modules. It is the most sufficient configuration when comparing mass, volume and cost [27, 28]. In this study, the total voltage in the FC system was $\geq 26 \text{ V}$; thus the voltage for every cell unit is $\geq 0.65 \text{ V}$. This setting prevents rapid wear of the FC stack. A potential of 26 V was thus used for the experiments. Figure 3(a) depicts power curves at different hydrogen stoichiometries at 55 °C and a hydrogen chemical dose of 1.4. The system was operated at a maximum power of 2.25 kW at 86.6 A and 26 V. The curves show no marked changes in performance as the hydrogen concentration increased at 55 °C. At a hydrogen stoichiometry of 2.0, the power reached 84.84 A–26 V. The curves also suggest wear and tear during the reaction of hydrogen, which are probably due to the sudden increase in the reaction rate with the increase in the amount of water. Attainment of maximum power by the FC system enabled hoisting of the load, but the amount of hydrogen used had to be reduced to allow use of the system for an extended period. The curves also indicate that a hydrogen stoichiometry of 1.4 at 55 °C is required for best performance of the stack. Figure 3(b) shows curves obtained at 60 °C. Similarly, the best performance was achieved at a hydrogen stoichiometry of 1.4. Under this condition, the maximum operating power reached 2.24 kW at 86.4 A and 26 V. When the temperature increased, the hydrogen flow rate increased to 1.2 and the power increased from 76.44 A–26 V to 84.98 A–26 V. Both changes substantially improved the performance, despite that the hydrogen flow rate was slightly lower than of 1.4. In addition, the stack performance was slightly lower than that at 55 °C. The increase in temperature probably increased the reaction rate, but it simultaneously produced more water and in turn decreased the reaction rate. This phenomenon may explain the best

performance achieved at a hydrogen flow rate of 1.4 at 60 °C. Figure 3(c) shows curves obtained at of 65 °C. Similarly, the best performance was observed at a hydrogen flow rate of 1.4. The maximum operating power reached 2.194 kW at 84.42 A and 26 V. At this flow rate, there was hardly any difference between the performance achieved at hydrogen flow rates of 1.2 and 1.6 (0.14 A–26 V power). When the temperature increased, a lower hydrogen flow rate resulted in better performance. However, a higher flow rate did not enhance the reaction of hydrogen. The reaction rate was limited because the temperature was too high and thus tended to decrease the reaction rate. Thus, the best performance was achieved at a hydrogen stoichiometry of 1.4 at a temperature of 65 °C.

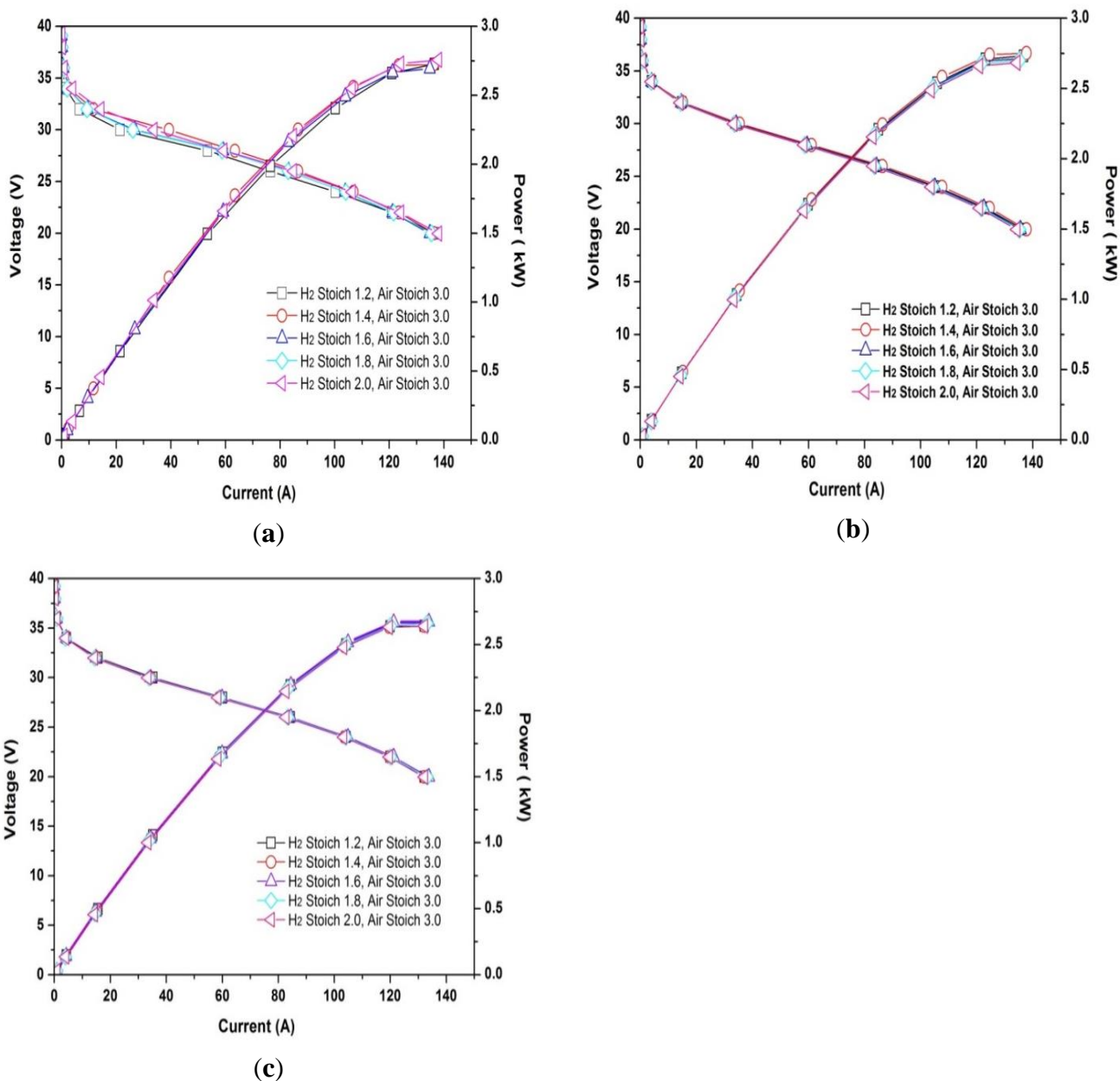


Figure 3. IV–IP curves for the stacks at different hydrogen flow rates at (a) 55 °C, (b) 60 °C, and (c) 65 °C

As shown in Figure 3, the optimum hydrogen flow rate (1.4) was applied to the anode terminal. The stack performance at different air flow rates was also investigated. Figure 4 depicts the stack performance at 55, 60, and 65 °C at air flow rates of 2.6, 2.8, and 3.0. In contrast to the air stoichiometries at 60 and 65 °C, the air stoichiometry at 55 °C is lower than 3.0 at all parameters, resulting in an optimum of 86.59 A–26 V. At an air stoichiometry of 2.6, a higher temperature resulted in better performance because a temperature increase accelerated the reaction between oxygen and air.

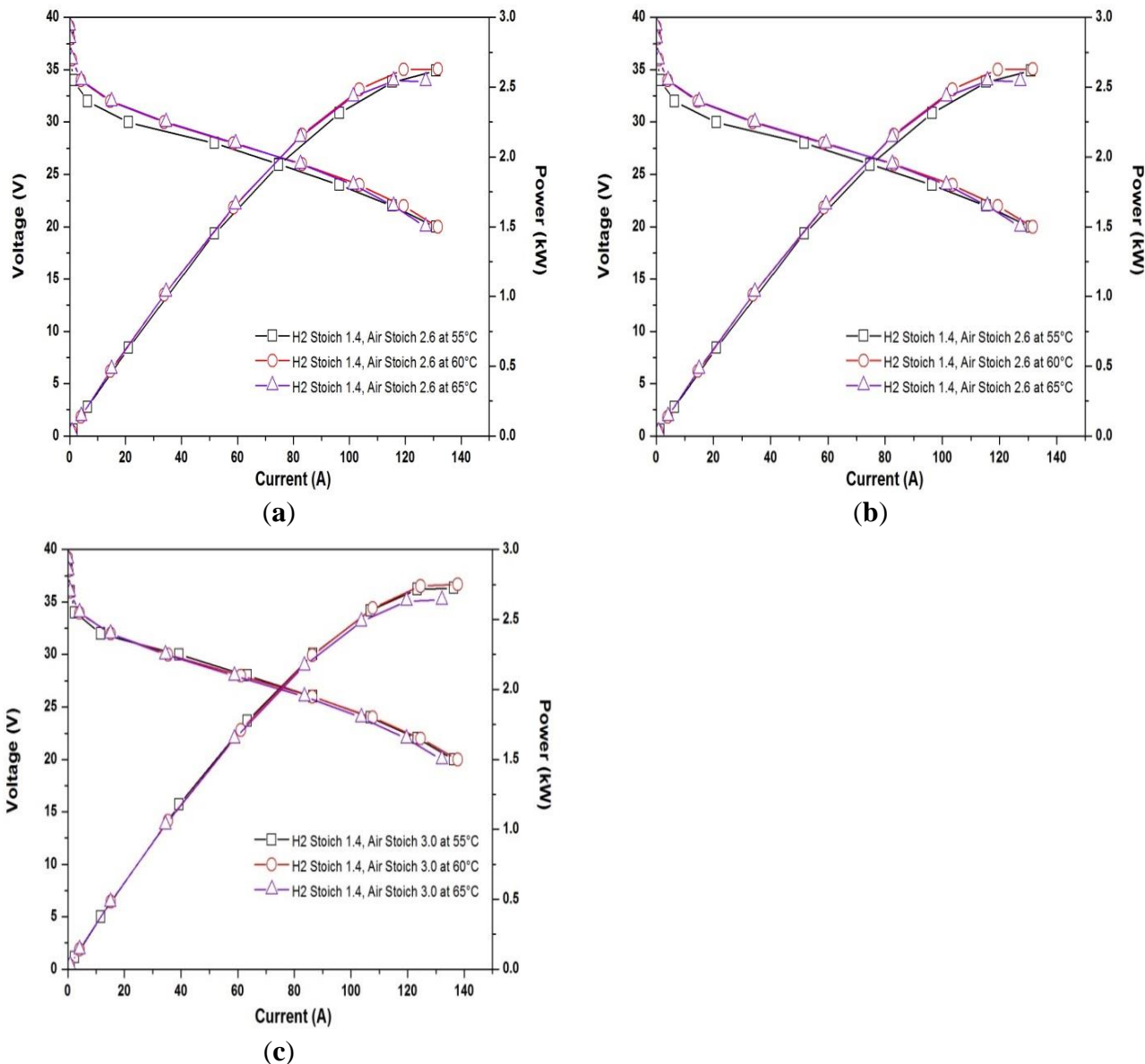


Figure 4. IV–IP curves for the stacks at different temperatures and at varying hydrogen and air stoichiometries.

At an air stoichiometry of 2.8, the performance declined at higher temperature. Under this condition, the high temperature of reaction increased performance, but the air stoichiometry was

insufficient. Therefore, the optimum operating conditions are a hydrogen stoichiometry of 1.4, an air stoichiometry of 3.0, and a temperature of 55 °C. These results are compared with those of previous studies. Su *et al.* [29] showed the polarization and power plots of the YZFC-OA stack at different H₂ stoich ratios of 1.6, 1.8 and 2.0 at room temperature. The air fans were operated at 9.0 V. When the stack was operated at stoich 1.8, the stack reached a maximum power output of 367 W at 45 A. Besides, stack performance increases slightly as air flow rate (fan voltage) was increased from 7.5 V to 9 V. In previous studies, the optimum operating temperature of a conventional PEMFC is generally regarded as being in the range of 60–80 °C [30, 31].

3.2. Experimental test on the lithium ion battery

Figure 5 shows the results of the discharge test for the lithium ion battery. The voltage in the discharge test was within 23–28 V. Farouk *et al.* [32] showed that the battery voltage is the same as the DC bus voltage, which should fit the converters voltage ratings. A 10-cell lithium-ion battery is used with a nominal voltage of 37 V (3.7 V for one battery cell). The supercapacitor cell is operated within the voltage range 1.35–2.7 V, so with 18 cells in series the voltage range is about 24–48 V, which fits as well the used DC/DC converters. As shown in Figure, 1C was found to discharge at 1100 mA/min. Theoretical values for the discharge times of 1C, 3C, and 5C are 60, 20, and 20 min, respectively. However, the measured discharge times are 55, 18, and 10 min. According to the manufacturer of the batteries, using the batteries within 40%–80% state of charge can prolong their lifetime during charge–discharge cycles.

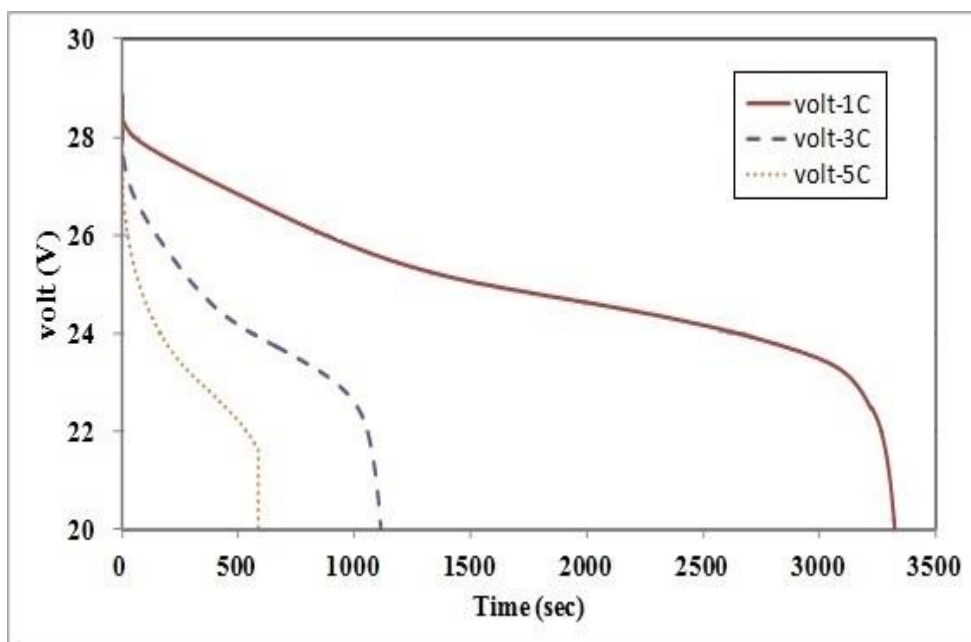


Figure 5. Voltages of the lithium ion batteries 1C, 3C, and 5C discharged for different periods

3.3. FC and energy storage devices

Figure 6 shows results of the final test for the overall system during carriage simulation. Operation stages of the vehicle may be divided into driving, climbing, and lifting. The overall state and the FC power changed as the load changed with the use of the auxiliary power supply control at 1.5 kW. It took 0 to 60 s to allow the entire system to reach equilibrium. The recharged lithium ion battery for the supercapacitor reached equilibrium in about 16 s in Part B, and it took 60–120 s to simulate the walking state. This observation is consistent with the ultracapacitance balance of the FC power output and continuous discharge, that is, lithium ion batteries continuously charge the supercapacitors to maintain balance. From 126 to 129 s at the maximum output, the supercapacitor could discharge more than 1.5 kW, thus protecting the FC and maintaining a fixed output during driving. The 160–300 s interval simulates climbing and corresponds to the FC maximum output retention of 1.5 kW. The other lithium ion battery and supercapacitor could serve as auxiliary power supply. At 360–400 s in the simulated lifting operation, switching to the lifting mode of Part B caused the supercapacitor to provide >2.0 kW of the power. At this stage, continuous lifting involved Part A ultracapacitors and lithium batteries which provided supporting power to maintain stable output of the FC system. Keränen et al. [33] designed and developed a triple-hybrid power system comprising a fuel cell system, an ultracapacitor module, and a lead-acid battery pack for an electric forklift. They showed that hybridization with the battery or capacitor could reduce the variation of the fuel cell and meet all power requirements. During sudden changes in the load, the ultracapacitor bank supplies the transient power demand successfully. Its fast response fulfills the power demand and increases the hybrid system power density [34].

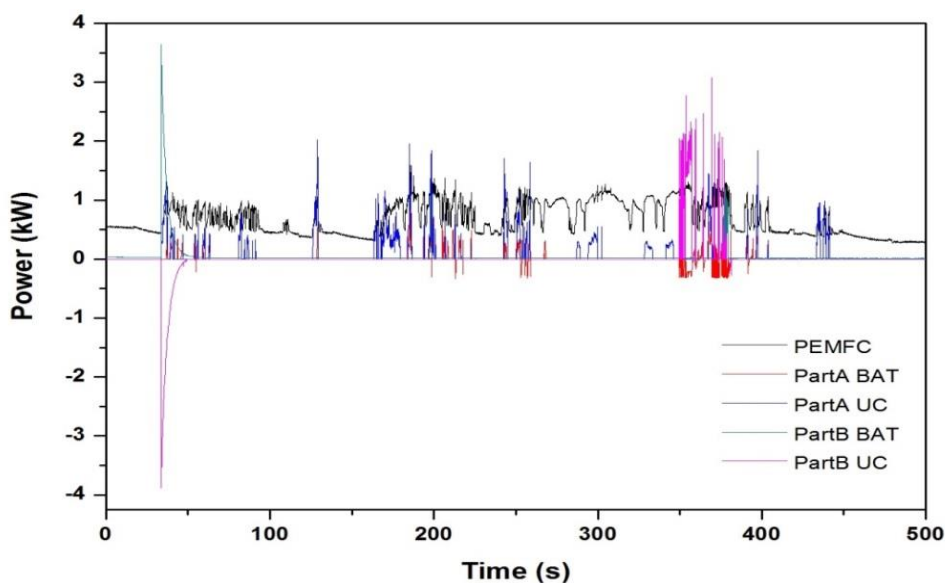


Figure 6. The output power for states at different times

Figure 7 displays the overall total output power for the truck. Simulation tests showed that a driving output power of 1.5–2.0 kW is sufficient for operation and that an output power of 3.5 kW is enough for instant acceleration. Climbing requires a large power source, that is, one with an average output power of 2.5–3.0 kW. Climbing with a load requires an even greater power source. Lifting as a whole demands a maximum output power of at least 3.0 kW. Figure 6 shows that the overall output power is positive, implying that the FC is fully capable of supporting the overall output. This design therefore meets all of the requirements for the operations of the electric pallet truck.

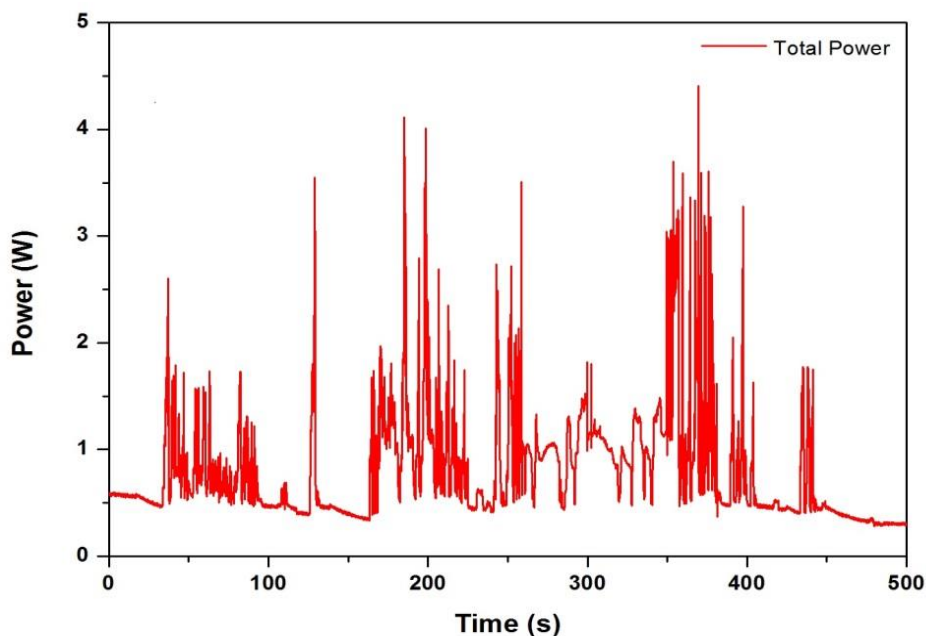


Figure 7. Total output power of the state

4. CONCLUSION

The key objective of the present work was to build a hybrid power-supply system for electric forklifts. A combination of batteries and supercapacitors with high energy and high power density comprises a suitable hybrid system. Our study examined a system consisting of a PEMFC, battery, and supercapacitor, taking into account the intrinsic energetic characteristics of these sources (i.e., energy and power densities and typical operating dynamics) under the energy management strategy. Such strategy prevents fast power transition and reduces stress in the FC and battery and thus extends the lifetime of the hybrid power source. We designed a system consisting of 2.5 kW FCs as the main body, and a lithium battery and supercapacitor with a total output of >4 kW. This system is sufficient for most pallet trucks and reduces the cost. It also facilitates manipulation of the wattage of the FC, thereby reducing overall system cost. In the literature, few studies have designed ultracapacitors for power supply systems, and some have set independently of the lifting end. The wattage of the FC must be increased to supply power for lifting the load. This increases the cost of upgrading or causes premature wear of the FC. Hence, an alternative solution is needed to supply power for lifting

operations. Our experimental results, which were obtained by using a small-scale test bench, a PEMFC, and storage devices composed of a supercapacitor and lithium battery module, corroborate the good performance of the proposed energy management system for the motor drive cycle. During motor starts and stops or at other significant steps of load transfer, the storage elements balance the energy needed by these operations.

ACKNOWLEDGEMENTS

The authors gratefully acknowledge the financial support from the Taiwan Asia-Pacific Fuel Cells program (contract FCS-W-150-036) and the Fuel Cell Center, Yuan Ze University.

Conflicts of interest

The authors declare no conflict of interest.

References

1. J. I. San Martin, I. Zamora, J. J. San Martin, V. Aperribay, E. Torres and P. Eguia, *Energy*, 35 (2010) 1898.
2. J. G. Carton, A. G. Olabi, *Energy*, 35 (2010) 4536.
3. Park Sehkyu, N. Popov Branko, *Fuel*, 88 (2009) 2068.
4. Therdthianwong Apichai, Saenwiset Pornrumpa and Therdthianwong Supaporn, *Fuel*, 91 (2012) 192.
5. J. Kurtz, K. Wipke, S. Sprik, T. Ramsden, C. Ainscough and G. Saur, Spring 2011 composite data products ARRA material handling equipment (ODE), Technical report, Department of Energy, U.S., 2011.
6. Todd Ramsden, An evaluation of the total cost of ownership of fuel cell-powered material handling equipment (ODE), Technical report, Department of Energy, U.S., 2013.
7. Haroune Aouzellag, Kaci Ghedamsi and Djamel Aouzellag, *Int. J. of Hydrogen Energy*, 40 (2015) 7204.
8. T.M. Keränen, H. Karimäki, J. Viitakangas, J. Vallet, J. Itonen, P. Hyötylä, H. Uusaloa and T. Tingelöf, *J. Power Sources*, 196 (2011) 9058.
9. Hassan Fathabadi, *Energy Conversion and Management*, 103 (2015) 573.
10. Vincenzo Liso, Mads Pagh Nielsen, Søren Knudsen Kær and Henrik H. Mortensen, *Int. J. of Hydrogen Energy*, 39 (2014) 8410.
11. B.L. Casolari, M.A. Ellington, J.M. Oros, P. Schuttinger, C.J. Radley, K.A. Kiley and L.E. Klebanoff, *Int. J. of Hydrogen Energy*, 39 (2014) 10757.
12. Ira Bloom, Lee K. Walker, John K. Basco, Thomas Malkow, Antonio Saturnio, Giancarlo De Marco and Georgios Tsotridis, *J. Power Sources*, 243 (2013) 451.
13. Azadeh Kheirandish, Mohammad Saeed Kazemi and Mahidzal Dahari, *Int. J. Hydrogen Energy*, 39 (2014) 13276.
14.] Islem Lachhab and Lotfi Krichen, *Int. J. Hydrogen Energy*, 39 (2014) 571.
15. A. Elgowainy, L. Gaines and M. Wang, *Int. J. Hydrogen Energy*, 34 (2009) 3557.
16. P. Agnolucci, *Int. J. Hydrogen Energy*, 32 (2007) 4306.
17. L. Andrzej and G. Maciej, *J. Power Sources*, 173 (2007) 822.
18. O.A. Ahmed and J.A.M Bleijs, *Renewable and Sustainable Energy Reviews*, 42 (2015) 609.
19. Qi Li, Weirong Chen, Zhixiang Liu, Ming Li and Lei Ma, *J. Power Sources*, 279 (2015) 267.
20. B. Vural, A.R. Boynuegri, I. Nakir, O. Erdinc, A. Balikci, M. Uzunoglu, H. Gorgun and S.

- Dusmez, *Int. J. Hydrogen Energy*, 35 (2010) 11161.
21. M.C. Kisacikoglu, M. Uzunoglu and M.S. Alam, *Int. J. Hydrogen Energy*, 34 (2009) 1497.
 22. Billy Wu, Michael A. Parkes, Vladimir Yufit, Luca De Benedetti, Sven Veismann, Christian Wirsching and et al., *Int. J. Hydrogen Energy*, 39 (2014) 7885.
 23. Phatiphat Thounthong, Stephane Raël and Bernard Davat, *J. Power Sources*, 193 (2009) 376.
 24. Yuedong Zhan, Youguang Guo, Jianguo Zhu and Li Li, *Int. J. Electrical Power & Energy Systems*, 67 (2015) 598.
 25. P. Thounthong, S. Raël and B. Davat, *J. Power Sources*, 158 (2006) 806.
 26. P. Rodatz, G. Paganelli, A. Sciarretta and L. Guzzella, *Control Eng. Pract.*, 13 (2005) 41.
 27. E. Schaltz, S.J. Andreasen and P.O. Rasmussen, Proceeding of the EPE 2007 – 12th European Conference on Power Electronics and Applications, Aalborg, Denmark, 2–5 September 2007, 1–10.
 28. A. Stepanov, I. Galkin and L. Bisenieks, Proceeding of the EPE 2007–12th European Conference on Power Electronics and Applications, Aalborg, Denmark, 2–5 September 2007, 1–7.
 29. Z.M. Huang, A. Su, C.J. Hsu and Y.C. Liu, *Fuel*, 122 (2014) 76.
 30. Kandlikar SG and Z. Lu, *Appl. Thermal Engineering*, 29 (2009) 1276.
 31. S. Kreitmeier, M. Michiardi, A. Wokaun and FN Büchi, *Electrochim Acta*, 80 (2012) 240.
 32. O. Farouk, R. Jürgen and H. Angelika, *Energies*, 8 (2015) 6302.
 33. T.M. Keränen, H. Karimäki, J. Viitakangas, J. Vallet, J. Ihonen, P. Hyötylä, H. Uusalo and T. Tingelöf, *J. Power Sources*, 196 (2011) 9058.
 34. B. Vural, A.R. Boynuegri, I. Nakir, O. Erdinc, A. Balikci, M. Uzunoglu, H. Gorgun and S. Dusmez, *Int. J. Hydrogen Energy*, 35 (2010) 11161.